Title
Canonical microRNAs in thymic epithelial cells promote central tolerance

Permalink
https://escholarship.org/uc/item/1xx1z20f

Journal
European Journal of Immunology, 44(5)

ISSN
0014-2980

Authors
Khan, Imran S
Taniguchi, Ruth T
Fasano, Kayla J
et al.

Publication Date
2014-05-01

DOI
10.1002/eji.201344079

Peer reviewed

Canonical microRNAs in thymic epithelial cells promote central tolerance

Imran S. Khan[1], **Ruth T. Taniguchi**[1], **Kayla J. Fasano**[1], **Mark S. Anderson**[1], and **Lukas T. Jeker**[1,2]

[1]Diabetes Center, University of California, San Francisco, CA, USA

[2]Departments of Medicine and Pathology, University of California, San Francisco, CA, USA

Abstract

Medullary thymic epithelial cells (mTECs) facilitate the deletion of developing self-reactive T cells by displaying a diverse repertoire of tissue-specific antigens, a process which largely depends on the expression of the autoimmune regulator (Aire) gene. Mature microRNAs (miRNAs) that regulate gene expression post-transcriptionally are generated in a multistep process. The microprocessor complex, including DGCR8, cleaves canonical miRNAs, but alternative DGCR8-independent miRNA biogenesis pathways exist as well. In order to study the role of canonical miRNAs in thymic epithelial cells (TECs), we ablated *Dgcr8* using a *FoxN1-Cre* transgene. We report that DGCR8-deficient TECs are unable to maintain proper thymic architecture and exhibit a dramatic loss of thymic cellularity. Importantly, DGCR8-deficient TECs develop a severe loss of Aire[+] mTECs. Using a novel immunization approach to amplify and detect self-reactive T cells within a polyclonal TCR repertoire, we demonstrate a link between the loss of *Aire* expression in DGCR8-deficient TECs and the breakdown of negative selection in the thymus. Thus, DGCR8 and canonical miRNAs are important in TECs for supporting central tolerance.

Keywords

Aire; Central tolerance; DGCR8; MicroRNAs; Thymic epithelial cells

Introduction

Thymic epithelial cells (TECs) support T-cell development in two distinct stages. Cortical thymic epithelial cells (cTECs) facilitate the positive selection of thymocytes that have undergone TCR rearrangements capable of recognizing self-MHC [1]. Positively selected thymocytes undergo negative selection by medullary thymic epithelial cells (mTECs) to eliminate self-reactive T cells [2]. To prevent autoimmunity, mTECs display a diverse repertoire of tissue-specific antigens (TSAs) whose expression is otherwise restricted to

correspondence: Dr. Lukas T. Jeker, UCSF Diabetes Center and Department of Pathology, University of California, San Francisco Box 0540, 513 Parnassus Ave., HSW 1002B, San Francisco, CA 94143-0540, USA, Fax: +1-415-564-5813, ljeker@diabetes.ucsf.edu.

Additional supporting information may be found in the online version of this article at the publisher's web-site

Conflict of interest: The authors declare no financial or commercial conflict of interest.

peripheral tissues [3–5]. Developing thymocytes bearing a TCR recognizing the TSAs undergo apoptosis to purge the developing T-cell pool of self-reactive T cells [6-8]. TSA expression in mTECs is largely dependent on autoimmune regulator (Aire), which is expressed in a subset of mature mTECs expressing high levels of MHC II and the costimulatory molecule CD80 [5, 9, 10]. Both patients and mice with mutations in *Aire* develop multiorgan autoimmunity which underscores the importance of TSA expression for the elimination of self-reactive T cells in maintaining tolerance [3, 11, 12].

MicroRNAs (miRNAs) are ~22 nucleotide-long noncoding RNAs that mediate sequence-dependent post-transcriptional gene repression [13, 14]. The primary miRNA transcripts of canonical miRNAs are processed by a complex formed by DROSHA and DGCR8 to generate ~60–80 nucleotide hairpin precursor miRNAs. After export to the cytoplasm, these hairpins are further processed by the RNase III enzyme Dicer to produce mature miRNAs. However, Dicer does not exclusively process miRNA precursors but rather includes a variety of small RNAs such as endogenous siRNAs, endogenous shRNAs, mirtrons, and Alu RNAs [15–17]. By ablating key genes required for miRNA biogenesis, we and others have previously demonstrated the importance of miRNAs in various lymphocyte populations [18–22]. Similarly, Dicer is important for TEC biology [23–25]. However, since Dicer is not restricted to processing miRNAs it remains unclear whether TEC development and function are truly dependent on the canonical miRNA pathway [15–17].

To further define the role of canonical miRNAs in TECs, we generated mice with TEC-specific deletion of *Dgcr8*, a component of the miRNA-specific microprocessor complex [16, 26]. Here, we find that DGCR8 is critical for maintaining the proper expression of *Aire* and the overall architecture of the thymic medulla. Furthermore, we demonstrate a breakdown in thymic negative selection in these animals by detecting pathogenic autoreactive T-cell clones in the periphery that are normally deleted in the thymus. Thus, proper thymic architecture and central tolerance depend on canonical miRNAs expressed in TECs.

Results and discussion

Thymic architecture and TEC composition depend on miRNAs

To study the role of canonical miRNAs in TEC function we first analyzed *Dgcr8* expression in mTECs and cTECs from C57BL/6J WT mice and found no significant differences in expression (data not shown). We then utilized *FoxN1-Cre* knock-in mice, which express Cre recombinase in all TECs without disrupting FoxN1 function, to conditionally inactivate *Dgcr8* in TECs (*Dgcr8* [TEC]) [26, 27]. We used qPCR analysis to verify that the deletion of *Dgcr8* in *Dgcr8* [TEC] mice was comparable between mTECs and cTECs (data not shown). At 2 weeks of age *Dgcr8* [TEC] mice exhibited evidence of disrupted thymic architecture with a loss of the distinct keratin-8 (K8) and keratin-5 (K5) staining patterns as compared with the characteristic separation between cortex and medulla in littermate control mice (Fig. 1A). The TECs in *Dgcr8* [TEC] mice appeared to be thinned out and many expressed both keratin markers (K5[+]K8[+]), a feature characteristic of immature TECs [28]. Though Aire^{+} cells were detectable at 2 weeks by immunofluorescent staining, they appeared to be reduced in number. By 6 weeks of age the *Dgcr8* [TEC] thymi had further deteriorated and

developed large patches lacking K5/K8 staining (Fig. 1A). Aire$^+$ cells were further depleted and nearly all remaining TECs were K5$^+$K8$^+$. H&E staining revealed confluent cellularity, demonstrating that the absence of K5/K8 staining did not represent a general absence of cells (e.g. a liquid filled cyst) but rather a specific loss of TEC or TEC identity (Fig. 1A).

To quantify and further characterize these changes in thymic architecture we performed flow cytometry on TECs. As expected from the histologic analysis, overall TEC cellularity was significantly reduced in 2-week-old *Dgcr8* $^{\text{TEC}}$ mice and further decreased by 6 weeks of age (Fig. 1B and Supporting Information Fig. 1A). Although *Dgcr8* $^{\text{TEC}}$ mice showed increased frequencies and absolute numbers of cTECs at 2 weeks of age, cTEC numbers were comparable to those of littermate controls by 6 weeks. In contrast, mTEC cellularity was reduced by nearly 80% in 2-week-old *Dgcr8* $^{\text{TEC}}$ mice and progressed to a 95% loss by 6 weeks (Fig. 1B). Within the mTEC compartment in 2-week-old mice, the relative frequency of Aire$^+$ cells was reduced while the immature mTEC$^{\text{lo}}$ (MHC II$^{\text{low}}$ Aire$^-$) and the more mature mTEC$^{\text{hi}}$ (MHC II$^{\text{hi}}$ Aire$^-$) cell subsets were relatively enriched (Fig. 1C) [9, 10]. In contrast, absolute cell numbers were reduced across all mTEC subsets at both 2-week and 6-week time points (Fig. 1D). However, the loss was most prominent in the Aire$^+$ cells. Thus, proliferating immature mTEC precursors could be partially compensating for the loss of the most mature mTECs. Supporting this notion, increased frequencies of the relatively enriched mTEC$^{\text{lo}}$ and mTEC$^{\text{hi}}$ cell subsets expressed the proliferation marker Ki67 (Fig. 1D). By 6 weeks of age, both mTEC$^{\text{hi}}$ and Aire$^+$ cells were relatively depleted in *Dgcr8* $^{\text{TEC}}$ mice while the mTEC$^{\text{lo}}$ subset was enriched. Similar to the 2-week time point, a larger proportion of mTEC$^{\text{lo}}$ cells expressed the proliferation marker Ki67 (Fig. 1D). Thus, increased proliferation rates of mTEC precursor cells partially compensated for the loss of the more differentiated mTECs.

To investigate whether the loss of Aire$^+$ mTEC resulted from the TEC-intrinsic loss of *Dgcr8* expression in mTEC or was an indirect consequence of disturbed TEC-thymocyte cross-talk we analyzed neonatal mice. While overall thymocyte cellularity was comparable between *Dgcr8* $^{\text{TEC}}$ and control mice 2 days postnatally, *Dgcr8* $^{\text{TEC}}$ mice exhibited a significant loss of both mTEC and cTEC cellularity (Supporting Information Fig. 2 A–E). The mTEC loss was specific to the mature mTEC$^{\text{hi}}$ and Aire$^+$ subsets, which is indicative of an initial TEC-intrinsic maturation defect in the thymi of *Dgcr8* $^{\text{TEC}}$ mice. Additional impaired TEC-thymocyte cross-talk may occur at later time points.

Together, these findings demonstrate that DGCR8-dependent canonical miRNAs are essential for TEC cellularity and mTEC maturation, particularly the accumulation and maintenance of *Aire*-expressing mTECs. This suggests that the histologically apparent mTEC voids in 6-week-old mice represent a true absence of mTECs. In addition, the altered relative TEC composition suggests a superimposed differentiation defect in which the mature mTEC$^{\text{hi}}$ and Aire$^+$ mTEC subsets are diminished while the immature mTEC$^{\text{lo}}$ cells accumulate and exhibit increased proliferation. These findings are consistent with the increased presence of K5$^+$K8$^+$ cells in *Dgcr8* $^{\text{TEC}}$ thymic sections suggesting that the loss of the most differentiated mTEC may trigger a proliferative response in immature TECs to compensate for the overall loss of TEC cellularity.

miRNAs are required for the maintenance of thymocyte cellularity

The profoundly altered thymic architecture and TEC cellularity suggested that thymocyte development could be affected by TEC-specific miRNA-deficiency. Thymi from 6- to 8-week old $Dgcr8$ [TEC] mice showed a significant reduction of over 60% in thymic cellularity (Fig. 2A). In contrast, the relative frequencies of CD4−CD8− double negative, CD4+CD8+ double positive, CD4+ single positive, CD8+ single positive thymocytes, and CD4+Foxp3+ Treg cells were not affected in $Dgcr8$ [TEC] mice. As a consequence, absolute numbers of all thymocyte developmental stages were proportionally reduced. These results suggest that although $Dgcr8$ [TEC] mice have a severely disrupted thymic architecture and significant reduction in TECs, the remaining TECs are sufficient to support T-cell development. This finding is reminiscent of Smad4-deficient TEC that lead to substantial thymic hypoplasia but intact relative thymocyte development [29]. Thus, the thymus appears to have a remarkable ability to maintain thymocyte development despite severely impaired TEC numbers and composition. Next, we analyzed whether the reduction of thymic T-cell numbers resulted in peripheral T-cell lymphopenia. In contrast to the thymic cellularity, total splenic cellularity was not different between $Dgcr8$ [TEC] and control mice, and CD4+ and CD8+ T-cell numbers were only modestly reduced (Fig. 2B). Thus, homeostatic proliferation in the periphery most likely compensated for the reduced thymic cellularity. However, despite the relatively normal thymocyte development and the presence of substantial numbers of T cells in lymph nodes and spleen, we could not exclude that the thymocytes developing in a $Dgcr8$ [TEC] microenvironment were functionally impaired or had a skewed TCR repertoire due to defective thymocyte selection. Indeed, mice with $Dicer$-deficient TECs develop collagen-induced arthritis with increased incidence but decreased severity suggesting both an altered T-cell repertoire and possibly impaired T-cell function [23]. Thus, $Dicer$-deficient TEC are not able to support numerically and functionally normal thymocyte development.

miRNA deficiency in TECs causes a breakdown in central tolerance

Given the complex consequences on T cells developing in $Dicer$-deficient TEC [23] and the prominent and progressive loss of Aire+ mTECs we sought to determine whether $Dgcr8$ [TEC] mice had a defect in central tolerance. $Dgcr8$ [TEC] mice did not develop spontaneous autoimmunity as evidenced by immune infiltrates in various organs or the presence of autoantibodies when compared with littermate controls, even when aged out beyond 45 weeks (data not shown). These findings are consistent with previous work which found that $Aire$ expression during the perinatal period is sufficient to induce central tolerance [30]. In addition, similar results have been reported for mice with $Dicer$-deficient TECs [25]. In these studies, depletion of T cells at 2 weeks of age to allow the seeding of potentially autoreactive T cells developing in a $Dicer$-deficient TEC microenvironment led to multiorgan autoimmune disease after 30 weeks [25]. Thus, the presence of some Aire+ TECs during the perinatal period, peripheral $Aire$ expression, and other peripheral tolerance mechanisms likely cooperated to prevent the development of spontaneous autoimmunity in $Dgcr8$ [TEC] mice [5, 31].

We hypothesized that although $Aire$ expression is partially maintained in young $Dgcr8$ [TEC] mice, self-reactive T cells could have escaped thymic deletion due to the disturbance of thymic architecture and the progressive loss of Aire+ mTECs, but be kept in check by

peripheral tolerance mechanisms. We aimed at testing this hypothesis in the polyclonal T-cell repertoire employing a novel approach to expand and detect Aire-dependent autoreactive T cells. In previous work, we determined that IRBP-specific T cells are normally deleted efficiently in the thymus of Aire-sufficient hosts and that such cells escape deletion in Aire-deficient thymi and provoke autoimmune uveitis [6]. Utilizing a previously described tetramer enrichment protocol, we developed methods to detect T cells with this specificity in the polyclonal repertoire of Aire-deficient hosts [8, 32]. Thus, we hypothesized that escaped self-reactive IRBP-specific CD4$^+$ T cells could be detected in $Dgcr8$ ^{TEC} mice given the loss of proper $Aire$ expression in these mice. To expand T cells for detection, we immunized $Dgcr8$ ^{TEC} and control mice with a MHC II binding IRBP peptide epitope (P2) and 10 days later pooled lymph nodes and spleen to enumerate CD4$^+$ P2-I-A^b-reactive T cells. Consistent with the loss of Aire$^+$ mTECs, immunized $Dgcr8$ ^{TEC} mice showed a significant expansion of P2-specific CD4$^+$ T cells when compared with littermate controls (Fig. 3A and Supporting Information 1B). Importantly, this expansion was also associated with a breakdown in immune tolerance with the generation of IRBP-specific autoantibodies and autoimmune uveitis in immunized $Dgcr8$ ^{TEC} mice when compared with control mice (Fig. 3B-C).

Concluding remarks

In summary, we show here that $Dgcr8$ expression in TECs is critical for the maintenance of proper corticomedullary thymic architecture and that canonical miRNAs are unequivocally required to support both TEC and thymocyte cellularity. miRNAs are critical for TEC differentiation and composition and for the development and maintenance of Aire$^+$ mTECs. Using a novel immunization approach to expand and detect autoreactive T cells in a polyclonal TCR repertoire, we demonstrate that TECs rely on miRNAs to prevent a breakdown in central tolerance. Furthermore, we show that immunization with self-antigen followed by tetramer-mediated detection of expanded self-reactive T-cell clones can be used as an effective and rapid tool to screen for central tolerance defects in animal models. Thus, such an approach may be useful to screen for hidden central tolerance defects in large scale mutagenesis projects.

Materials and methods

Mice

FoxN1-Cre knock-in mice were kindly provided by N. Manley [27]. Floxed $Dgcr8$ mice were kindly provided by R. Blelloch [26]. $IRBP^{-/-}$ mice were described previously [6]. Throughout this study, $Dgcr8$ ^{TEC} represents $B6.FoxN1-Cre^+$ $Dgcr8^{fl/fl}$ mice and littermate controls are both $B6.FoxN1-Cre^+$ $Dgcr8^{fl/+}$ mice and all $B6.FoxN1-Cre^-$ mice. Mice were housed and bred under specific-pathogen free conditions at the University of California, San Francisco (UCSF) Animal Barrier Facility. Animal experiments were approved by the Institutional Animal Care and Use Committee (IACUC) at UCSF.

Histology and immunofluorescence

Thymi were harvested and embedded in Tissue-Tek Optimal Cutting Temperature media. Eight micrometer frozen thymic sections were fixed in 100% acetone and blocked in 10% goat serum before incubation with primary antibodies. Primary antibodies were purchased from either Abcam (keratin-5, keratin-8) or eBioscience (Aire) and all secondary antibodies were purchased from Invitrogen. Immunofluorescence slides were visualized using a Zeiss Apotome widefield microscope. For eye disease scoring, eyes were processed by formalin fixation and H&E staining as previously described [6, 8]. Sections were blindly scored for severity of infiltration and tissue destruction. H&E slides were imaged using a Zeiss AxioImager brightfield microscope.

Flow cytometry

Thymic stromal cells were isolated as previously described [33]. Briefly, thymi were minced with razor blades and digested with DNase I and Liberase TM (Roche) before gradient centrifugation with Percoll PLUS (GE Healthcare). Enriched stromal cells were blocked with the Fc-receptor blocking antibody 2.4 G2 and stained with the indicated surface marker antibodies (BioLegend). For intracellular staining with anti-Aire-A647 (eBiosciences) and anti-Ki67-PE (BD Biosciences), cells were stained using the Foxp3 Staining Buffer Set (eBiosciences). For staining of lymphocytes, all surface marker antibodies were obtained from BioLegend except anti-Foxp3-APC, which was obtained from eBiosciences. Flow cytometry was performed using a LSR II flow cytometer (BD Biosciences), and raw data were analyzed using FACS Diva (BD Biosciences) and Flow Jo (Tree Star).

Immunization

As described previously, 7- to 8-week old mice were immunized subcutaneously with 100 μg of P2 peptide emulsified in 100 μL of CFA [8]. For induction of autoimmune uveitis, mice were given an i.p. injection of 400 ng pertussis toxin at the time of immunization. Mice were harvested 10 days following immunization for tetramer analysis and 21 days following immunization for uveitis analysis.

Tetramer analysis

P2-I-A^b tetramer (Interphotoreceptor retinol binding protein 3, amino acids 294–306) was generated by the NIH Tetramer Core Facility, and tetramer staining was performed according to previously described protocols [8, 32]. Briefly, mice were harvested 10 days following immunization and lymphocytes were pooled from lymph nodes and spleen. Cells were stained with tetramer for 1 hour at room temperature and enriched for tetramer+ cells using anti-APC microbeads and MACS columns (Miltenyi Biotech). Positively selected cells were stained with antibodies for flow cytometry, and counting beads (Invitrogen) were used to enumerate tetramer+ cells.

Generation of ^{35}S-radiolabeled IRBP and autoantibody assay

The autoantibody assay was described previously [7]. Briefly, full-length cDNA for mouse IRBP (Thermo Scientific, #MMM1013) was used for in vitro transcription and translation and labeling with ^{35}S-methionine using the TNT system kit (Promega). The ^{35}S-IRBP was

immunoprecipitated with serum samples in 96-well PVDF filtration plates (Millipore). Serum samples were analyzed in triplicate with 20 000 cpm of ^{35}S-IRBP per well. Radioactivity of immunoprecipitated material was evaluated with a liquid scintillation counter (1450 MicroBeta TriLux, Perkin Elmer). Serum samples from $Aire^{+/+}$ and $Aire^{-/-}$ mice were used as negative and positive standards, respectively (data not shown). The IRBP autoantibody index for each serum sample was found by the following calculation: (cpm in unknown sample–cpm in negative standard) ÷ (cpm in positive standard–cpm in the negative standard) × 100).

Statistical analysis

Statistical analysis was performed using Prism 6.0 (Graph-pad). Mann–Whitney testing was performed for tetramer analysis, autoantibody indices, and histological analyses. Student's t-test was performed for TEC and lymphocyte analyses. *denotes p 0.05, **denotes p 0.01, and ***denotes p 0.001.

Supplementary Material

Refer to Web version on PubMed Central for supplementary material.

Acknowledgments

References

1. Starr TK, Jameson SC, Hogquist KA. Positive and negative selection of T cells. Annu Rev Immunol. 2003; 21:139–176. [PubMed: 12414722]

2. Kyewski B, Klein L. A central role for central tolerance. Annu Rev Immunol. 2006; 24:571–606. [PubMed: 16551260]

3. Anderson MS, Venanzi ES, Klein L, Chen Z, Berzins SP, Turley SJ, von Boehmer H, et al. Projection of an immunological self shadow within the thymus by the Aire protein. Science. 2002; 298:1395–1401. [PubMed: 12376594]

4. Derbinski J, Schulte A, Kyewski B, Klein L. Promiscuous gene expression in medullary thymic epithelial cells mirrors the peripheral self. Nat Immunol. 2001; 2:1032–1039. [PubMed: 11600886]

5. Metzger TC, Anderson MS. Control of central and peripheral tolerance by Aire. Immunol Rev. 2011; 241:89–103. [PubMed: 21488892]

6. DeVoss J, Hou Y, Johannes K, Lu W, Liou GI, Rinn J, Chang H, et al. Spontaneous autoimmunity prevented by thymic expression of a single self-antigen. J Exp Med. 2006; 203:2727–2735. [PubMed: 17116738]

7. Shum AK, DeVoss J, Tan CL, Hou Y, Johannes K, O'Gorman CS, Jones KD, et al. Identification of an autoantigen demonstrates a link between interstitial lung disease and a defect in central tolerance. Sci Transl Med. 2009; 1:9ra20.

8. Taniguchi RT, DeVoss JJ, Moon JJ, Sidney J, Sette A, Jenkins MK, Anderson MS. Detection of an autoreactive T-cell population within the polyclonal repertoire that undergoes distinct autoimmune

regulator (Aire)-mediated selection. Proc Natl Acad Sci U S A. 2012; 109:7847–7852. [PubMed: 22552229]

9. Gabler J, Arnold J, Kyewski B. Promiscuous gene expression and the developmental dynamics of medullary thymic epithelial cells. Eur J Immunol. 2007; 37:3363–3372. [PubMed: 18000951]

10. Gray D, Abramson J, Benoist C, Mathis D. Proliferative arrest and rapid turnover of thymic epithelial cells expressing. Aire J Exp Med. 2007; 204:2521–2528.

11. Consortium FGA. An autoimmune disease, APECED, caused by mutations in a novel gene featuring two PHD-type zinc-finger domains. Nat Genet. 1997; 17:399–403. [PubMed: 9398840]

12. Nagamine K, Peterson P, Scott HS, Kudoh J, Minoshima S, Heino M, Krohn KJ, et al. Positional cloning of the APECED gene. Nat Genet. 1997; 17:393–398. [PubMed: 9398839]

13. Bartel DP. MicroRNAs: target recognition and regulatory functions. Cell. 2009; 136:215–233. [PubMed: 19167326]

14. Kim VN, Han J, Siomi MC. Biogenesis of small RNAs in animals. Nat Rev Mol Cell Biol. 2009; 10:126–139. [PubMed: 19165215]

15. Babiarz JE, Hsu R, Melton C, Thomas M, Ullian EM, Blelloch R. A role for noncanonical microRNAs in the mammalian brain revealed by phenotypic differences in Dgcr8 versus Dicer1 knockouts and small RNA sequencing. RNA. 2011; 17:1489–1501. [PubMed: 21712401]

16. Babiarz JE, Ruby JG, Wang Y, Bartel DP, Blelloch R. Mouse ES cells express endogenous shRNAs, siRNAs, and other Microprocessor-independent, Dicer-dependent small RNAs. Genes Dev. 2008; 22:2773–2785. [PubMed: 18923076]

17. Suh N, Baehner L, Moltzahn F, Melton C, Shenoy A, Chen J, Blelloch R. MicroRNA function is globally suppressed in mouse oocytes and early embryos. Curr Biol. 2010; 20:271–277. [PubMed: 20116247]

18. Baumjohann D, Kageyama R, Clingan JM, Morar MM, Patel S, de Kouchkovsky D, Bannard O, et al. The microRNA cluster miR-17~92 promotes TFH cell differentiation and represses subset-inappropriate gene expression. Nat Immunol. 2013; 14:840–848. [PubMed: 23812098]

19. Jeker LT, Bluestone JA. Small RNA regulators of T cell-mediated autoimmunity. J Clin Immunol. 2010; 30:347–357. [PubMed: 20393792]

20. Jeker LT, Bluestone JA. MicroRNA regulation of T-cell differentiation and function. Immunol Rev. 2013; 253:65–81. [PubMed: 23550639]

21. Jeker LT, Zhou X, Blelloch R, Bluestone JA. DGCR8-mediated production of canonical micrornas is critical for regulatory T cell function and stability. PLoS One. 2013; 8:e66282. [PubMed: 23741528]

22. Zhou X, Jeker LT, Fife BT, Zhu S, Anderson MS, McManus MT, Bluestone JA. Selective miRNA disruption in T reg cells leads to uncontrolled autoimmunity. J Exp Med. 2008; 205:1983–1991. [PubMed: 18725525]

23. Papadopoulou AS, Dooley J, Linterman MA, Pierson W, Ucar O, Kyewski B, Zuklys S, et al. The thymic epithelial microRNA network elevates the threshold for infection-associated thymic involution via miR-29a mediated suppression of the IFN-alpha receptor. Nat Immunol. 2012; 13:181–187. [PubMed: 22179202]

24. Ucar O, Tykocinski LO, Dooley J, Liston A, Kyewski B. An evolutionarily conserved mutual interdependence between Aire and microRNAs in promiscuous gene expression. Eur J Immunol. 2013; 43:1769–1778. [PubMed: 23589212]

25. Zuklys S, Mayer CE, Zhanybekova S, Stefanski HE, Nusspaumer G, Gill J, Barthlott T, et al. MicroRNAs control the maintenance of thymic epithelia and their competence for T lineage commitment and thymocyte selection. J Immunol. 2012; 189:3894–3904. [PubMed: 22972926]

26. Rao PK, Toyama Y, Chiang HR, Gupta S, Bauer M, Medvid R, Reinhardt F, et al. Loss of cardiac microRNA-mediated regulation leads to dilated cardiomyopathy and heart failure. Circ Res. 2009; 105:585–594. [PubMed: 19679836]

27. Gordon J, Xiao S, Hughes B 3rd, Su DM, Navarre SP, Condie BG, Manley NR. Specific expression of lacZ and cre recombinase in fetal thymic epithelial cells by multiplex gene targeting at the Foxn1 locus. BMC Dev Biol. 2007; 7:69. [PubMed: 17577402]

28. Klug DB, Carter C, Gimenez-Conti IB, Richie ER. Cutting edge: thymocyte-independent and thymocyte-dependent phases of epithelial patterning in the fetal thymus. J Immunol. 2002; 169:2842–2845. [PubMed: 12218095]

29. Jeker LT, Barthlott T, Keller MP, Zuklys S, Hauri-Hohl M, Deng CX, Hollander GA. Maintenance of a normal thymic microenvironment and T-cell homeostasis require Smad4-mediated signaling in thymic epithelial cells. Blood. 2008; 112:3688–3695. [PubMed: 18695001]

30. Guerau-de-Arellano M, Martinic M, Benoist C, Mathis D. Neonatal tolerance revisited: a perinatal window for Aire control of autoimmunity. J Exp Med. 2009; 206:1245–1252. [PubMed: 19487417]

31. Nurieva RI, Liu X, Dong C. Molecular mechanisms of T-cell tolerance. Immunol Rev. 2011; 241:133–144. [PubMed: 21488895]

32. Moon JJ, Chu HH, Hataye J, Pagan AJ, Pepper M, McLachlan JB, Zell T, et al. Tracking epitope-specific T cells. Nat Protoc. 2009; 4:565–581. [PubMed: 19373228]

33. Gardner JM, Devoss JJ, Friedman RS, Wong DJ, Tan YX, Zhou X, Johannes KP, et al. Deletional tolerance mediated by extrathymic Aire-expressing cells. Science. 2008; 321:843–847. [PubMed: 18687966]

Abbreviations

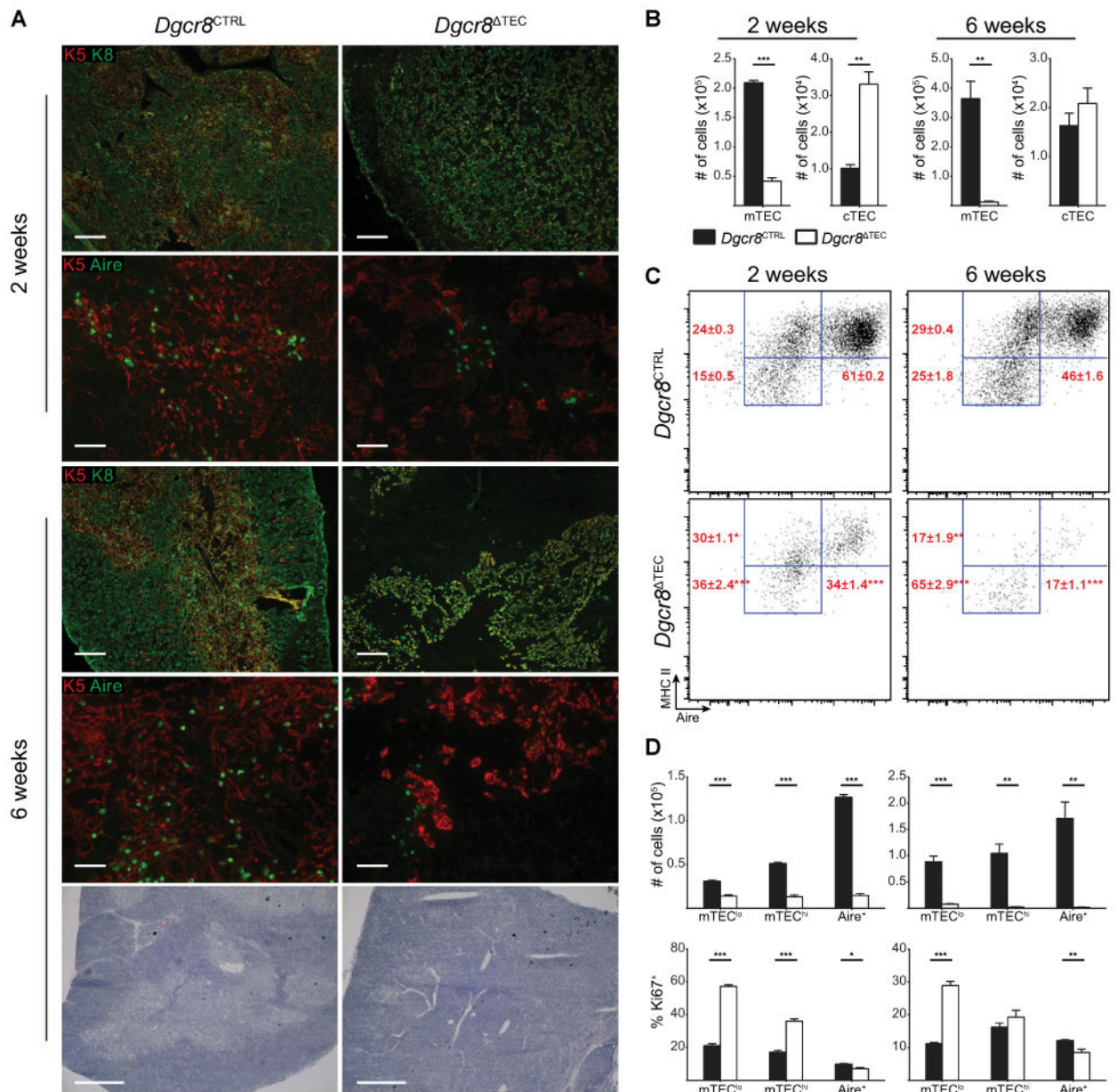|	
Aire	autoimmune regulator
miRNA	MicroRNA
TEC	thymic epithelial cell
cTEC	cortical thymic epithelial cell
mTEC	medullary thymic epithelial cell
TSA	tissue-specific antigen

Figure 1.
Thymic architecture and TEC composition depend on miRNAs. (A) Frozen thymic sections from $Dgcr8^{\Delta TEC}$ and littermate control mice were assessed for expression of keratin-5 (K5, red), keratin-8 (K8, green), and Aire (green) by immunofluorescent staining at indicated time points. Scale bars = 200 μm (K5 K8) and 50 μm (K5 Aire). The bottom panel shows H&E staining of indicated genotypes at the 6-week time point, scale bars = 500 μm. Data shown are representative images from two to three independent experiments. (B) Enumeration of total mTEC and cTEC cellularity by flow cytometry. cTECs were defined as CD45⁻, EpCAM⁺, Ly51⁺, MHC II⁺ events. mTECs were defined as CD45⁻, EpCAM⁺, Ly51⁻, MHC II⁺ events. (C) Subset composition was assessed by flow cytometry of mTECs as defined in (B). (D) Quantification of total TEC cellularity and assessment of the

proliferation marker Ki67 for the mTEC subsets shown in (C). mTEC subsets were defined as mTEC^{lo} (MHC II^{low}, Aire$^-$), mTEC^{hi} (MHC II^{hi}, Aire$^-$), and Aire$^+$ (MHC II^{hi}, Aire$^+$). White bars in (B) and (D) indicate *Dgcr8* ^{TEC} mice, black bars indicate littermate controls. Data shown in (B–D) are shown as mean + SEM of 3–10 samples and are representative of at least two independent experiments. * denotes p 0.05, ** denotes p 0.01, and *** denotes p 0.001, Student's *t*-test.
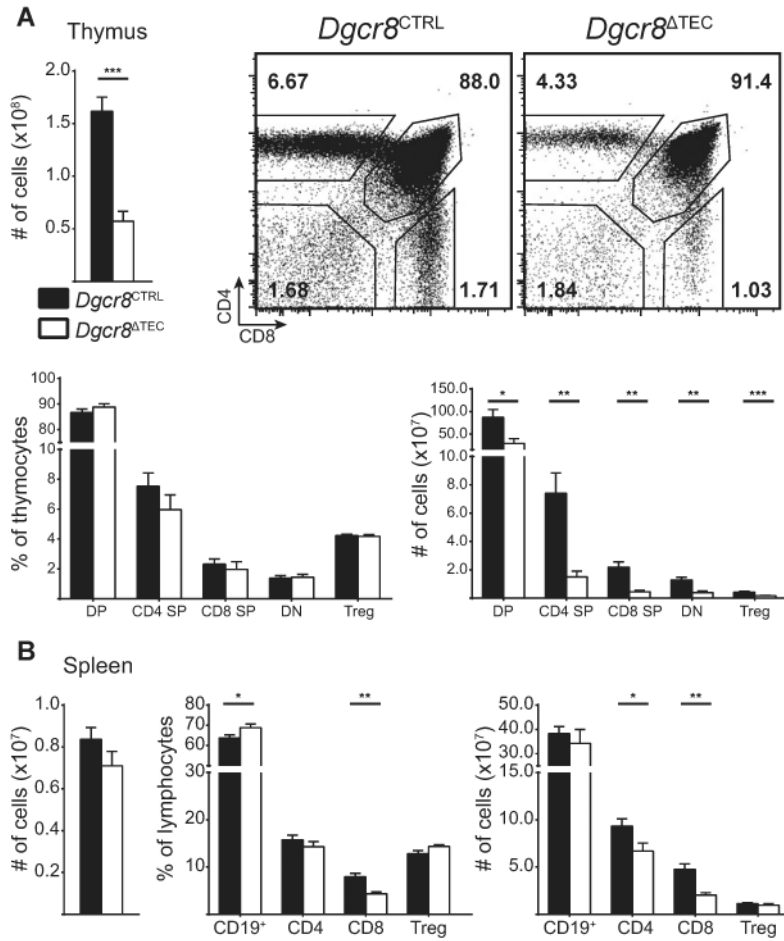
Figure 2.
miRNAs are required for the maintenance of thymocyte cellularity. (A) Total thymic cellularity from 6-week-old mice was assessed by flow cytometry. Plots show thymocyte subsets: CD4−CD8− double negative (DN), CD4+CD8+ double positive (DP), CD4+ single positive (SP), CD8+ SP thymocytes and CD4+Foxp3+ Treg cells. Relative frequencies are shown as a proportion of all thymocytes with the exception of Treg cells, which are shown as a proportion of CD4+ SP thymocytes. Total thymocyte data are shown as mean + SEM of 9–13 samples pooled from four independent experiments. Thymocyte subset data are shown as mean + SEM of 7–8 samples pooled from at least two independent experiments. (B) Total splenic cellularity from 6- to 8-week old mice. Indicated lymphocyte subsets are shown as a proportion of all splenocytes with the exception of Treg cells, which are shown as a proportion of CD4+ T cells. All splenocyte data are shown as mean + SEM of 7–11 samples pooled from four independent experiments. White bars in (A) and (B) indicate $Dgcr8^{\Delta TEC}$ mice, black bars indicate littermate controls. * denotes $p < 0.05$, ** denotes $p < 0.01$, and *** denotes $p < 0.001$, Student's t-test.
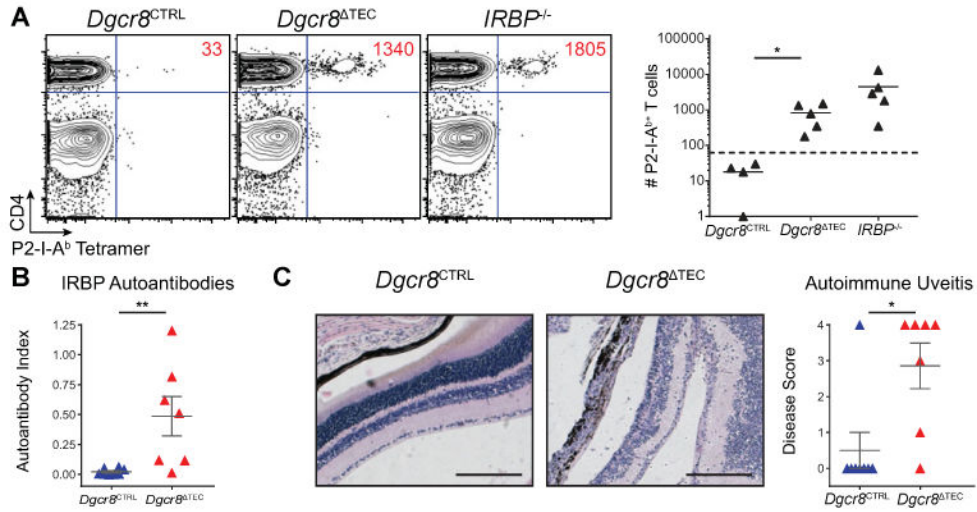
Figure 3.
miRNA deficiency in TECs causes a breakdown in central tolerance. (A) Mice were immunized with P2 peptide and then harvested 10 days later by flow cytometry following a tetramer pulldown assay. Plots are pregated on DAPI⁻, NK1.1⁻, CD11b⁻, CD11c⁻, F4/80⁻, B220⁻, CD3⁺ events. Absolute numbers of P2-specific cells are inset within the flow cytometry plots. Tetramer data are pooled from four to five samples in three independent experiments. *IRBP*⁻/⁻ mice were included as a positive control for immunization and tetramer pulldown. (B) The IRBP-specific immune response was assessed by an IRBP autoantibody assay in mice immunized with P2 peptide and harvested 21 days later. (C) Eyes harvested from mice in (B) were H&E stained and scored for infiltrates. Scale bars = 200 μm. Data in (B) and (C) is shown as mean ± SEM of 7–8 samples pooled from two independent experiments. * denotes *p* 0.05, and ** denotes *p* 0.01, Mann–Whitney test.